

Context-dependent neuronal differentiation and germ layer induction of *Smad4*^{-/-} and *Cripto*^{-/-} embryonic stem cells

Kai-Christian Sonntag,^{a,b} Rabi Simantov,^{a,b} Lars Björklund,^{a,b} Oliver Cooper,^{a,b} Jan Pruszk, ^{a,b} Florian Kowalke,^{a,b} Jocelyn Gilmartin,^{a,b} Jixiang Ding,^{c,d,e} Ya-Ping Hu,^{d,e} Michael M. Shen,^{d,e} and Ole Isacson^{a,b,*}

^aUdall Parkinson's Disease Research Center of Excellence, McLean Hospital/Harvard Medical School, Belmont, MA 02478, USA

^bNeuroregeneration Laboratories, McLean Hospital/Harvard Medical School, Belmont, MA 02478, USA

^cDepartment of Molecular, Cellular and Craniofacial Biology, Birth Defects Research Center, University of Louisville School of Dentistry, Louisville, KY 40202, USA

^dCenter for Advanced Biotechnology and Medicine, University of Medicine and Dentistry of New Jersey-Robert Wood Johnson Medical School, Piscataway, NJ 08854, USA

^eDepartment of Pediatrics, University of Medicine and Dentistry of New Jersey-Robert Wood Johnson Medical School, Piscataway, NJ 08854, USA

Received 31 December 2003; revised 10 March 2004; accepted 2 June 2004

Activation of transforming growth factor- β (TGF- β) receptors typically elicits mesodermal development, whereas inhibition of this pathway induces neural fates. In vitro differentiated mouse embryonic stem (ES) cells with deletion of the TGF- β pathway-related factors *Smad4* or *Cripto* exhibited increased numbers of neurons. *Cripto*^{-/-} ES cells developed into neuroecto-/epidermal cell types, while *Smad4*^{-/-} cells also displayed mesodermal differentiation. ES cell differentiation into catecholaminergic neurons showed that these ES cells retained their ability to develop into dopaminergic and serotonergic neurons with typical expression patterns of midbrain and hindbrain genes. In vivo, transplanted ES cells to the mouse striatum became small neuronal grafts, or large grafts with cell types from all germ layers independent of their ES cell genotype. This demonstrates that *Smad4*^{-/-} and *Cripto*^{-/-} ES cells favor a neural fate in vitro, but also express the mesodermal phenotype, implying that deletion of either *Smad4* or *Cripto* is not sufficient to block nonneuronal tissue formation.

© 2004 Elsevier Inc. All rights reserved.

Introduction

ES cells are pluripotent cells derived from the inner cell mass of preimplantation embryos (Evans and Kaufman, 1981; Martin, 1981). They can be maintained in vitro as immature cells, or

differentiated into specific cell types providing tools for analyzing cell development (Dinsmore et al., 1996; Hooper et al., 1987; Nagy et al., 1993) and potentially as a source for cell therapy (Björklund et al., 2002; Daley, 2002; Kim et al., 2002; Le Belle and Svendsen, 2002; Rossi and Cattaneo, 2002; Weissman, 2000). In an animal model of Parkinson's disease (PD), we have recently shown that wild-type ES cells transplanted into the striatum of parkinsonian rats can spontaneously differentiate into functional neurons (Björklund et al., 2002; Deacon et al., 1998). However, the pluripotent ES cells also developed into unwanted cell types derived from all different germ layers. Studies during the last decade have established that members of the transforming growth factor- β (TGF- β) superfamily play a critical role in cell morphogenesis and lineage specification in the developing brain (Munoz-Sanjuan and Brivanlou, 2001, 2002; Schier and Talbot, 2001). Thus, regulation of neuronal growth, differentiation, and specification depends on the activity of these growth and morphogenetic factors, their antagonists, as well as their target membrane-bound receptors and intracellular signaling proteins (Munoz-Sanjuan and Brivanlou, 2002; Tiedemann et al., 2001; Tropepe et al., 2001).

Smad4 and *Cripto* encode key components of the TGF- β signaling pathway that regulates multiple aspects of embryogenesis, including mesodermal and epidermal cell development (Bianco et al., 2002; Ding et al., 1998; Kimura et al., 2001; Massague and Chen, 2000; Minchiotti et al., 2002; Munoz-Sanjuan and Brivanlou, 2002; Persico et al., 2001; Sirard et al., 1998; Wrana, 2000; Yan et al., 2002; Yang et al., 1998) and it has been suggested that inhibition of these intrinsic and extrinsic signals can favor neuroectoderm development (Munoz-Sanjuan and Brivanlou, 2002). *Smad4*^{-/-} mice die before day 7.5 of embryogenesis, fail to

* Corresponding author. Neuroregeneration Laboratories, Harvard Medical School, MRC 120, McLean Hospital, 115 Mill Street, Belmont, MA 02478. Fax: +1 617 855 3284.

E-mail address: isacson@hms.harvard.edu (O. Isacson).

Available online on ScienceDirect (www.sciencedirect.com).

gastrulate or express mesodermal markers, and show abnormal visceral endoderm (Sirard et al., 1998; Weinstein et al., 2000; Yang et al., 1998). *Cripto*^{-/-} mice also die around day 7.5 of embryogenesis and have striking defects in mesoderm formation and axial organization (Ding et al., 1998). These embryos consist mostly of anterior neuroectoderm and lack posterior structures (head without trunk).

Based on these results, we hypothesized that knockout mutations in *Smad4* or *Cripto* would also redirect ES cell differentiation toward the neuroectodermal fate in vitro and in vivo. To this end, we analyzed the developmental profile of the *Smad4*^{-/-} stem cell line C8-13A1 (Sirard et al., 1998), its parent cell line E14K (Sirard et al., 1998), two *Cripto*^{-/-} cell lines (CHG51 and CHG79, J.D., Y.-P.H., and M.M.S., unpublished data), and their corresponding parental line TC1 in a five-stage in vitro differentiation protocol (Chung et al., 2002; Lee et al., 2000) and in transplantation experiments into the striatum of adult mice. The emphasis of the following experiments was to determine whether *Smad4*^{-/-} and *Cripto*^{-/-} ES cells favored neuronal cell

development, particularly in the generation of catecholaminergic neurons, and abrogate teratoma formation in vivo.

Results

Time course of in vivo differentiation of transplanted naïve ES cells into the brain

We have shown that wild-type ES cells [at ES and embryoid body (EB) stage] transplanted into the striatum of parkinsonian rats can spontaneously differentiate into functional neurons, but also developed into unwanted cell types derived from the different germ layers (Bjorklund et al., 2002; Deacon et al., 1998). Two types of graft morphologies were observed after cell transplantation in the striatum based on the final size with grafts smaller (<25 mm³) or bigger (>25 mm³) than striatum (Figs. 1A–D). Whereas small grafts had a homogenous cell density with almost exclusive neuronal cell development (Fig. 1A), large grafts developed into

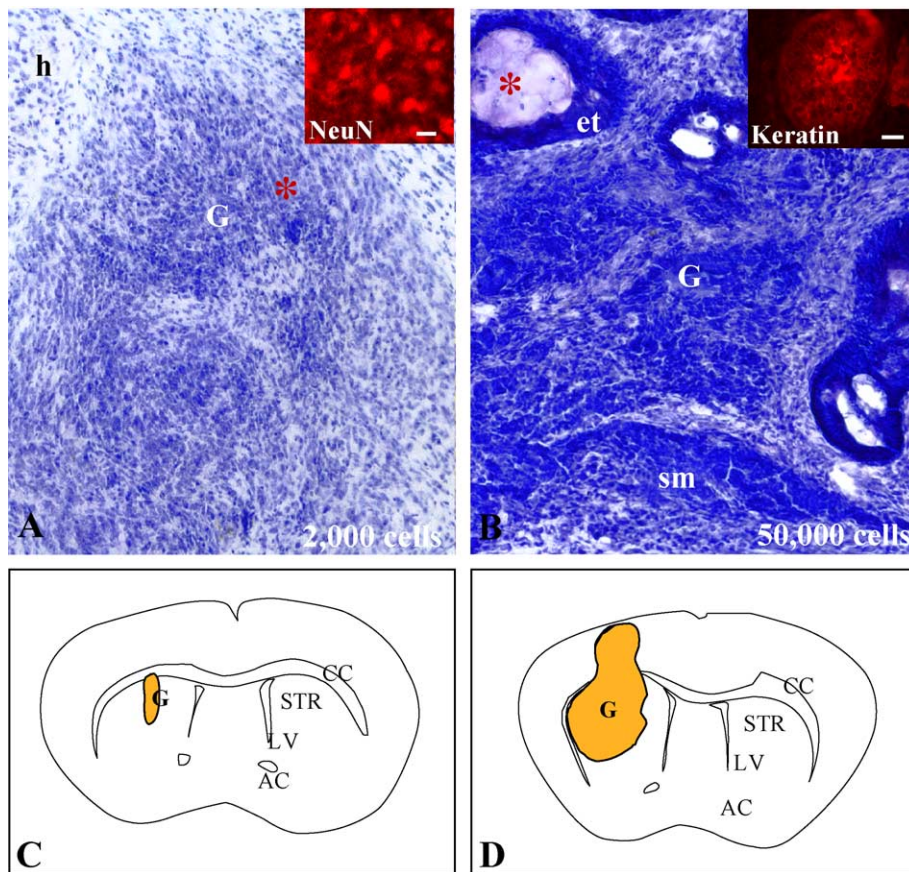


Fig. 1. Development of D3 ES cell grafts in the striatum. (A, B) Photomicrographs (20 × magnification) of hematoxylin and eosin stained sections from representative small (A) and large (B) mouse ES cell-derived grafts (G) in rat striatum. Small grafts mainly consisted of neurons as demonstrated by NeuN staining of a graft section marked by red asterisk (inset in A). h = host. Large grafts represent teratomas with cells from multiple lineages, such as smooth muscle (sm) and epithelial cells (et). The inset shows Keratin staining of an epithelial graft section marked by red asterisk. (C, D) Computer-assisted drawing of a small (C) and large (D) graft from brain sections using a stereology workstation. CC = corpus callosum; STR = striatum; LV = left ventricle; AC = anterior commissure; G = graft. (E, F) Stage-specific embryonic antigen 1 (SSEA1) (light green) staining of grafts at different time points after transplantation. Left and middle columns represent grafts of 2000 (E) and the right column of 50,000 ES cells (F). Samples were analyzed at low (5×) magnification. The inset shows a confocal image (40× magnification) of clusters of SSEA1⁺ cells (green) surrounded by developing Nestin⁺ neural precursors (red) in a graft of 2000 ES cells, 14 days after implantation. Cell nuclei are counterstained in blue using bisbenzimidazole dye. (G, H) Development of Tuj1⁺ neuronal cells. Representative ICC images of a Tuj1⁻ graft at 14 days (G) and a Tuj1⁺ graft at 28 days post transplantation (H). Scale bars = 200 μm. (K) Stereology-based quantification of SSEA1⁺ cells in grafts at different time points after transplantation. Green bars show results for 2000 and yellow bars for 50,000 transplanted cells.

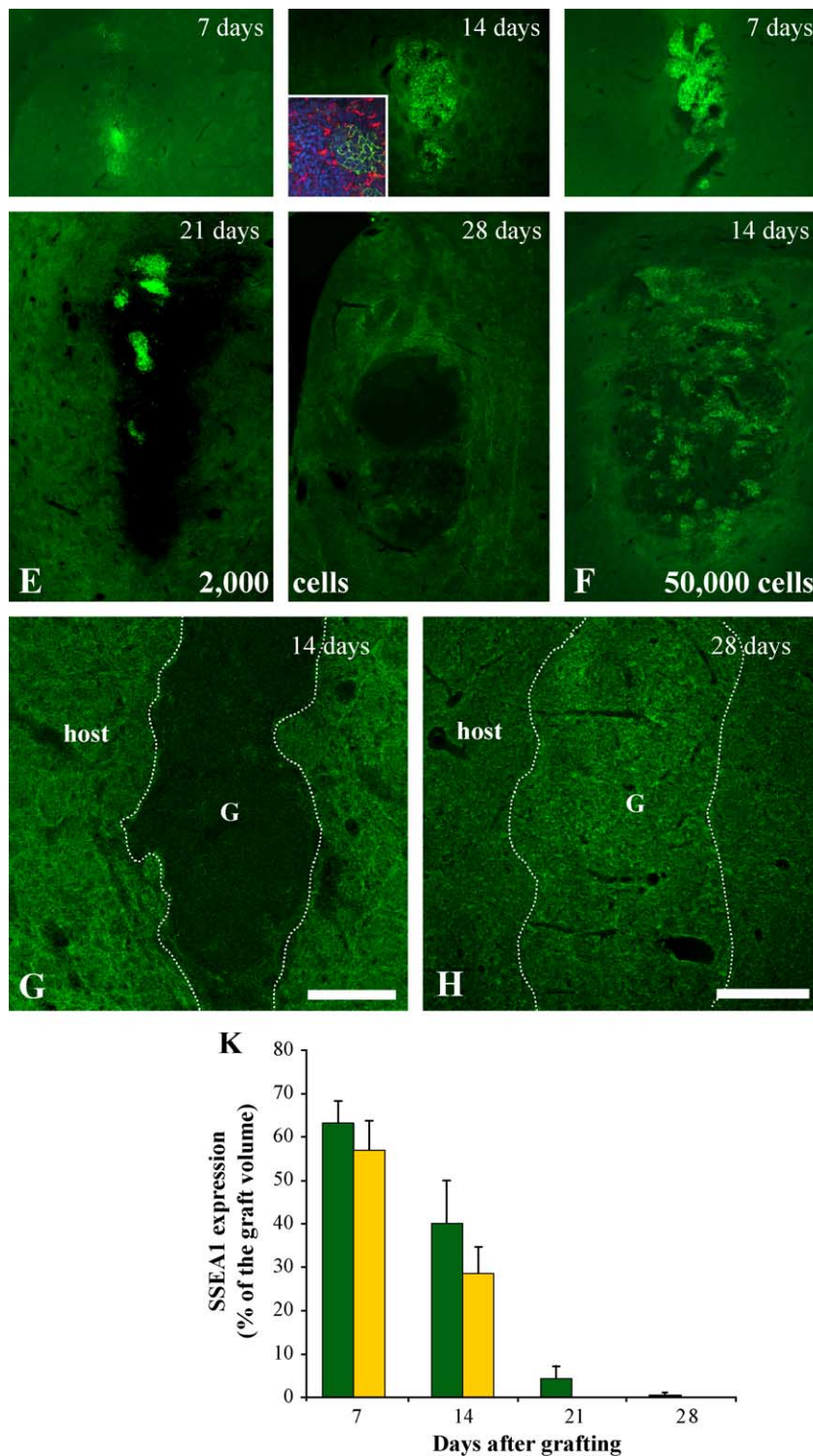


Fig. 1 (continued).

teratoma-like structures with cells from multiple lineages (Fig. 1B). Our results also indicated that large grafts preferentially developed at transplantation of high doses of ES cells (50×10^3), whereas a larger number of small grafts were found after transplantation of low ES cell doses (2×10^3). To further investigate possible

mechanisms involved in *in vivo* graft development, we performed time course analyses of ES cell grafts and compared the effects of high vs. low doses of ES cells transplanted into the animals. We found that small grafts had a significant portion of cells expressing the immature stem cell marker SSEA1 at 7 and 14 days post

transplantation (64% and 40%, respectively), which decreased to 5% and 1% after 21 and 28 days, respectively (Figs. 1E, F, and K). In the high dose grafts, the fraction of SSEA1 cells was 57% at 7 days and decreased to 28% at 14 days and all animals developed large teratoma-like grafts at 14 days post transplantation. We also found that Nestin⁺ neural precursor cells started to appear between 7 and 14 days (inset in Fig. 1E) and neuronal (Tuj1⁺) cells between 14 and 28 days post transplantation (Figs. 1G and H). These results indicate that transplantation of high doses of ES cells promote large teratoma-like graft development, whereas implantation of low ES cell numbers produced small neuronal-like grafts.

Gene expression profiles during in vitro differentiation of *Smad4*^{-/-} and *Cripto*^{-/-} ES cells

To determine the differentiation capacities of the *Smad4*^{-/-} and *Cripto*^{-/-} ES cells, we in vitro differentiated these cells and their corresponding WT cell lines using a five stage differentiation protocol (Chung et al., 2002; Lee et al., 2000) and analyzed gene expression profiles by semiquantitative RT-PCR at various stages of cell development (Figs. 2 and 3). Based on our hypothesis that the mutant cell lines show enhanced neurogenesis, we first determined neuronal gene expressions. When compared to the

WT ES cell line E14K, the *Smad4*^{-/-} cells showed an increase in Tuj1 expression at the end of the differentiation stages NP (stage 3, day 8) and ND (stage 5, day 15) (Figs. 2A and B). There was also an increased expression of Nestin and Tuj1 at the NP and ND cell stages in the *Cripto*^{-/-} ES cell line 79, and to a lower extent in line 51, when compared to the corresponding WT TC1 cells (Figs. 3A and B). In addition, we performed RT-PCR of marker genes relevant to the catecholaminergic and especially to the midbrain DA neuronal phenotype such as tyrosine hydroxylase (TH) and the transcriptional activator *Nurr1*. At all stages of cell development, the *Smad4*^{-/-} and *Cripto*^{-/-} cells had similar gene expression profiles of *Nurr1* and TH when compared with the WT E14K and TC1 ES cell lines, respectively (Figs. 2A and 3A). This was also true for other DA-specific marker genes such as L-amino acid decarboxylase (AADC), aromatic aldehyde-dehydrogenase (AHD2), and the dopamine transporter (DAT) (data not shown). In all cell lines, there was no expression of the noradrenergic marker dopamine β-hydroxylase (DBH) (data not shown).

Next, we analyzed the expression of transcription factors that play a developmental role at early embryonic stages within the midbrain–hindbrain territory and the ventral mesencephalon (Rhinn and Brand, 2001). We found that the gene expression profiles of the forebrain–midbrain marker *Otx2* and the rostral

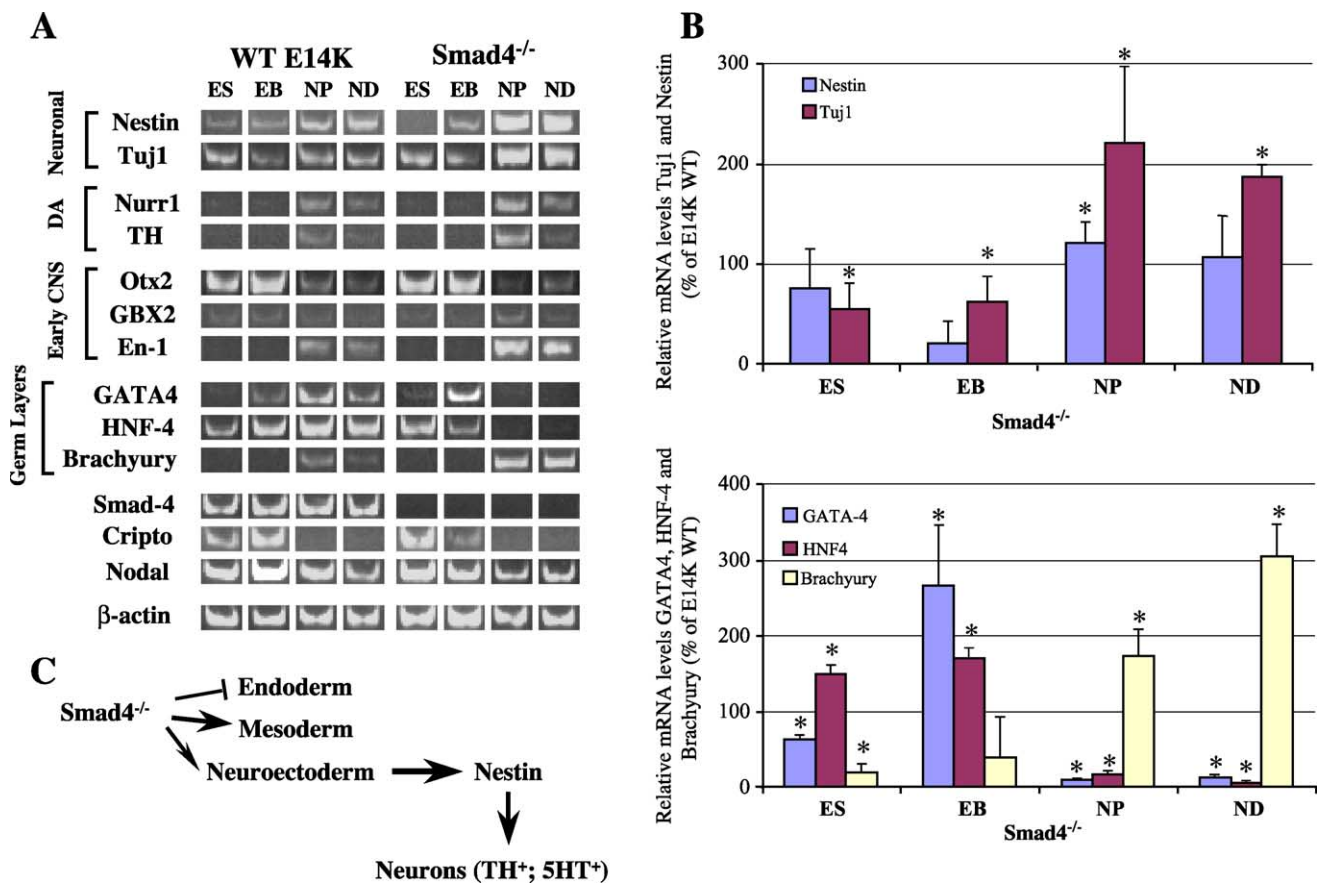


Fig. 2. Gene expression profiles of neuronal, DA, early CNS, germ layer, and TGF-β signaling pathway-related markers during and after in vitro differentiation of WT and *Smad4*^{-/-} ES cells. ES cells were in vitro differentiated as described (Chung et al., 2002; Lee et al., 2000). (A) Results of RT-PCR experiments performed at different stages of differentiation: ES = embryonic stem cells; EB = embryoid bodies; NP = selection of neural precursors; and ND = neural differentiation. (B) Semiquantitative analyses of *Smad4*^{-/-} RT-PCR signals for nestin and Tuj1 and GATA4, HNF4, and Brachyury. Results are plotted as percentages of corresponding signals from E14K WT samples (**P* < 0.05). (C) Interpretation of the RT-PCR results presented schematically. After in vitro differentiation, *Smad4*^{-/-} ES cells do not develop endodermal, but mesodermal phenotypes and neuroectodermal Nestin⁺ precursors as well as catecholaminergic (TH⁺, 5HT⁺) neurons (see Fig. 5).

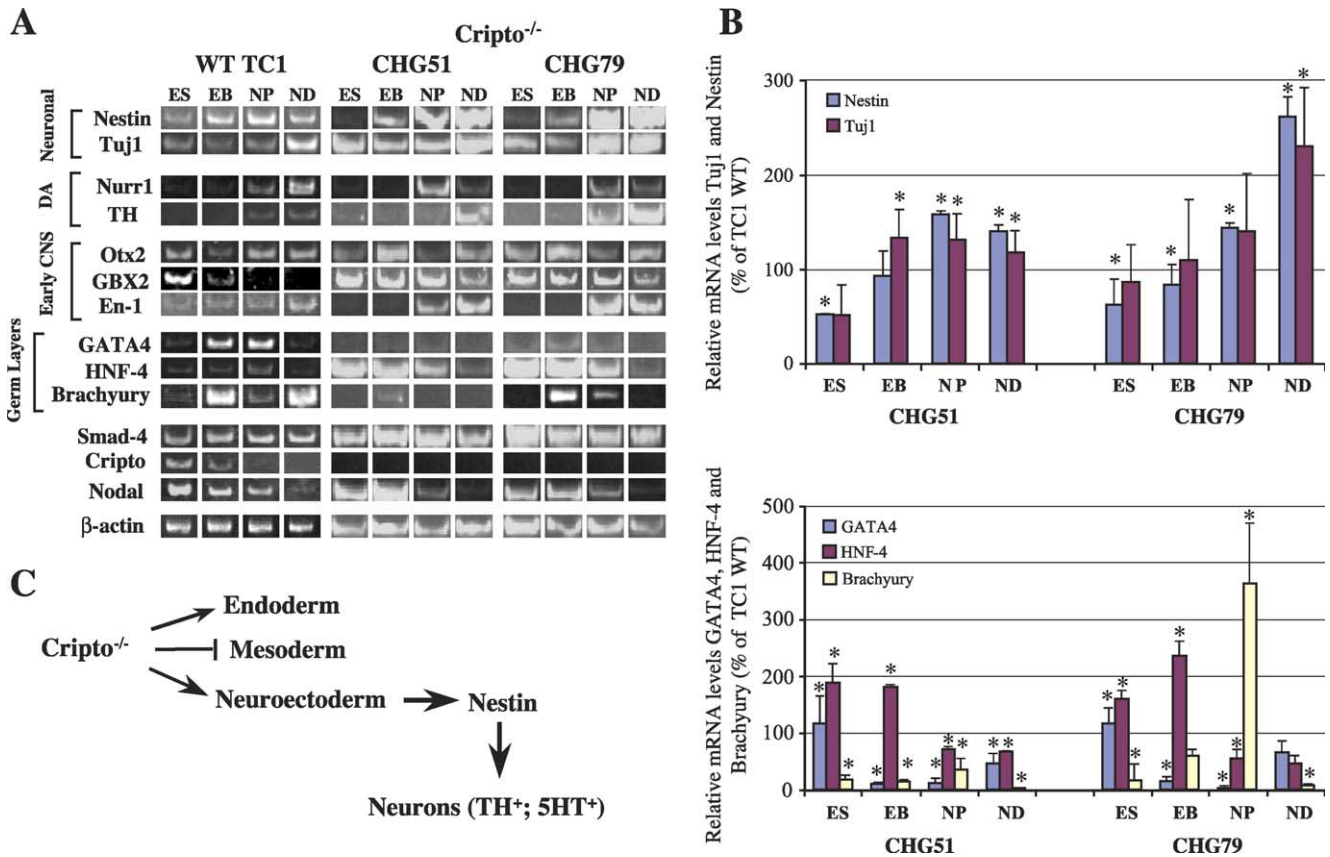


Fig. 3. Gene expression profiles of neuronal, DA, early CNS, germ layer, and TGF- β signaling pathway-related markers during and after in vitro differentiation of WT and *Cripto*^{-/-} ES cells. (A) Results of RT-PCR experiments performed at different stages of differentiation as described in legend of Fig. 2. Note that the *Cripto*^{-/-} ES cells lack early *En-1* (ES, EB) gene expression and up-regulate the rostral hindbrain marker *GBX2* at late stages (NP, ND) of cell development. (B) Semiquantitative analyses of the *Cripto*^{-/-} (clone CHG51 and CHG79) RT-PCR signals for nestin and Tuji1 and GATA4, HNF4, and Brachyury. Results are plotted as percentages of corresponding signals from TC1 WT samples (* $P < 0.05$). (C) Interpretation of the RT-PCR results presented schematically. In vitro differentiated *Cripto*^{-/-} ES cells develop early, but not late endodermal phenotypes at early (ES, EB, NP) stages of cell development. In contrast, they do not develop mesoderm at late stages, but neuroectodermal Nestin⁺ precursors as well as catecholaminergic (TH⁺, 5HT⁺) neurons (see Fig. 5).

hindbrain marker *Gbx2* were not different between the parent E14K and *Smad4*^{-/-} cells, whereas the midbrain- and anterior hindbrain-specific marker *En-1* was late upregulated in the knockout cell line (Fig. 2A). Interestingly, analysis of the WT TC1 cell line revealed late expression of *Otx2* and some early expression of *En-1* (Fig. 3A). There was no difference in the expression profile for *Otx2* between WT TC1 and *Cripto*^{-/-} cells. However, *Gbx2* was consistently upregulated in the two *Cripto*^{-/-} cell lines, whereas *En-1* was upregulated only in the NP and ND cell stages (Fig. 3A). These data suggest that in vitro, *Smad4*^{-/-} cells tended to express a more mid- and anterior hindbrain gene profile, whereas the *Cripto*^{-/-} cells also expressed rostral CNS gene markers.

In embryogenesis, mutation of *Smad4* and *Cripto* negatively influences mesoderm and definitive endoderm formation (Ding et al., 1998; Sirard et al., 1998; Yang et al., 1998). We therefore analyzed the expression of several marker genes that are related to germ layer formation such as the early endodermal transcription factor *GATA4* (Soudais et al., 1995), the late endodermal factor hepatic nuclear factor 4 (*HNF4*) (Li et al., 2000), and the visceral mesodermal marker *Brachyury* (Wilkinson et al., 1990) (Figs. 2A and 3A). It was apparent that the *Smad4*^{-/-} ES cells had no *GATA4* expression, a down-regulated

HNF4 and up-regulated *Brachyury* expression at late stages (NP and ND) of cell differentiation when compared to the parental E14K cell line (Figs. 2A and B). The *Cripto*^{-/-} cells had a down-regulation of *GATA4* and an early (ES, EB), but not late (NP, ND), increase in *HNF4* transcription when compared to the WT TC1 cell line (Figs. 3A and B). Interestingly, there was no late (ND) *Brachyury* expression in the *Cripto* mutant cells as seen in the TC1 cells. These data indicate that *Smad4*^{-/-} cells developed early mesoderm at late stages of in vitro differentiation. *Cripto*^{-/-} ES cells, however, showed some expression of endoderm markers at early stages of differentiation, which may reflect differentiation of extraembryonic visceral endoderm rather than definitive endoderm.

We also determined the expression profile of the *Smad4* and *Cripto* genes during ES cell differentiation. We found that *Smad4* was constitutively expressed through all five stages of in vitro differentiation in both WT TC1 and the *Cripto*^{-/-} cell lines (Fig. 3A), whereas *Cripto* expression appeared to be down-regulated at NP and ND stages in the WT E14K and *Smad4*^{-/-} cells (Fig. 2A). In all cell lines (WT and mutants), expression of *Nodal*, which encodes a transforming growth factor β (TGF- β -related factor that utilizes *Cripto* as a coreceptor (Bianco et al., 2002; Yan et al., 2002), was highly up-regulated early, and down-regulated late, at cell development (Figs. 2A and 3A).

Characterization of cell development after *Smad4*^{-/-} and *Cripto*^{-/-} ES cell differentiation

The results from the RT-PCR experiments showed that the *Smad4*^{-/-} and the *Cripto*^{-/-} lines had higher expression of the neuronal marker Tuj1, indicating an increase in neurogenesis. We therefore analyzed neuronal cell development after in vitro differentiation by ICC. We found that both the WT and the mutant cell lines grew in Tuj1⁺ cell clusters (Fig. 4A). Interestingly, in the parental ES cell line E14K, the Tuj1⁺ neurons were typically confined to small regions at the edge of these clusters. The density of Tuj1⁺ neurons at these edge regions was 35.5 ± 15.3 cells/field ($n = 23$), whereas the center of the clusters had only few Tuj1⁺ cells (1.2 ± 1.3 cells/field, $n = 20$). In contrast, the

majority of the clusters in the corresponding *Smad4*^{-/-} cultures contained Tuj1⁺ neurons distributed within and around the clusters, with an average of 42.2 ± 10.4 neurons/field ($n = 23$) (Fig. 4A). In the WT TC1 and the corresponding *Cripto*^{-/-} cells, there was a mixed distribution of clusters with Tuj1⁺ neurons in the periphery or in the center with no significant differences of amounts of Tuj1⁺ neurons between the three cell lines (data not shown). In addition to neurons, all cell lines also developed GFAP⁺ astrocytes (Fig. 5A).

Based on our hypothesis that the differentiation of *Smad4*^{-/-} and *Cripto*^{-/-} ES cells would limit the formation of mesodermal and/or epidermal cell types, we also performed immunocytochemistry using the markers Myosin (mesoderm) and Cytokeratin (ectoderm, epiderm) after in vitro differentiation (Fig. 4B). Cytokeratin⁺ cell populations were present in all cell lines. Myosin⁺ cells were present in the WT E14K and TC1 (59 ± 2.9 , $n = 20$ and 97 ± 4.9 , $n = 20$, respectively) and *Smad4*^{-/-} cell lines (73 ± 3.6 , $n = 20$), but were absent in the *Cripto*^{-/-} cell cultures (0 , $n = 40$). In addition, we analyzed the presence of immature cell types, such as Nestin⁺ neural precursors and stage-specific early antigen 1 (SSEA1)-positive immature stem cells (Fig. 4B). Both immature cell types were found in all cell cultures. Interestingly, there was a high proportion of SSEA1⁺ cells in the *Cripto*^{-/-} cell cultures (704 ± 35.2 , $n = 20$), when compared to the corresponding WT TC1 cultures (1 ± 0.3 , $n = 40$).

Development of catecholaminergic neuronal subtypes after *Smad4*^{-/-} and *Cripto*^{-/-} ES cell differentiation

The emphasis of our study was to determine whether the *Smad4*^{-/-} and/or *Cripto*^{-/-} ES cells could be useful as a tool for cell replacement therapy in neurodegenerative diseases, such as Parkinson's disease. We therefore analyzed the development of neuronal subtypes including tyrosine hydroxylase-positive (TH⁺)/Tuj1⁺ cells (Fig. 5A). Quantification revealed the presence of 4% TH⁺ neurons ($n = 22$) in both WT cell lines consistent with other results from WT ES cells (Chung et al., 2002; Lee et al., 2000). Notably, there was no significant difference in the percentage of TH⁺ neurons between the *Smad4*^{-/-} (3.6%, $n = 23$) and *Cripto*^{-/-} cell lines (0.1% and 1.7%, respectively; $n = 18$ and 16).

We also analyzed serotonergic (5-HT) neuronal cell development. WT E14K and the *Smad4*^{-/-} ES cell lines showed significant staining for serotonin (5HT⁺) in Tuj1⁺ neurons, which were also partly positive for the enzyme that synthesizes serotonin, tryptophane hydroxylase (TrH) (Fig. 5B). Similar staining patterns were observed for the *Cripto*^{-/-} cell lines CHG51 and CHG79 (data not shown). Quantification of the 5HT⁺ neurons showed that 58% ($n = 24$) of the WT and 52% ($n = 27$) of the *Smad4*^{-/-} cell clusters contained colonies of 8.5 ± 5.9 and 5.7 ± 2.9 5HT⁺ neurons per colony, respectively (Fig. 5B). Differentiation of both *Cripto*^{-/-} ES cell lines revealed significantly less 5HT⁺ neuronal cell clusters (<10%), however with a larger number of 5HT⁺ cells per colony (28.8 ± 15.9 $n = 50$).

In vivo differentiation of *Smad4*^{-/-} and *Cripto*^{-/-} ES cells

The in vitro differentiation experiments showed that *Cripto*^{-/-} cells, but not *Smad4*^{-/-} ES cells, have defects in terminal differentiation of some mesodermal cell types. We therefore analyzed the in vivo differentiation capacities of the *Smad4*^{-/-}, the *Cripto*^{-/-}, and the WT E14K ES cells. Because cell develop-

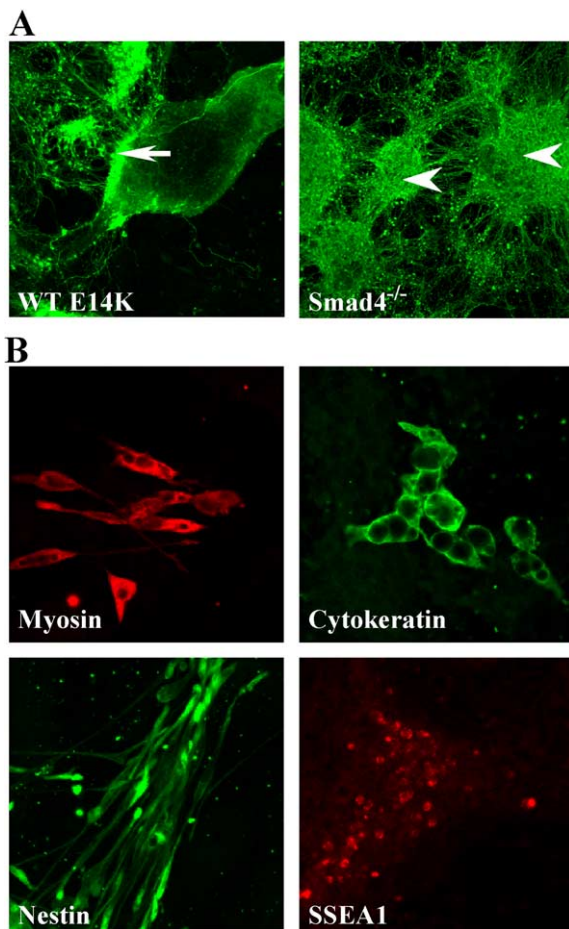


Fig. 4. Development of cellular phenotypes after in vitro differentiation of WT, *Smad4*^{-/-}, and *Cripto*^{-/-} ES cells. The WT E14K and TC1, *Smad4*^{-/-} (C8-13A1), and two *Cripto*^{-/-} ES cell lines (CHG51 and CHG79) were in vitro differentiated as described (Chung et al., 2002; Lee et al., 2000). (A) Differentiated neurons were stained with the neuronal-specific antibody Tuj1 (green) and cell cultures were analyzed at low magnification (10 \times) in fluorescence microscopy. Neurons grew in clusters and developed at the edge (arrows) or in the centers (arrow heads) of the clusters. (B) Mesodermal and ectodermal/epidermal cell development was determined by ICC with staining for Myosin (red, WT TC1) and Cytokeratin (green, *Cripto*^{-/-}), respectively (upper row). Nestin⁺ (green, WT TC1) and SSEA1⁺ (red, *Cripto*^{-/-}) cells after in vitro differentiation demonstrate the presence of immature cell populations (lower row). Samples were analyzed with 63 \times magnification.

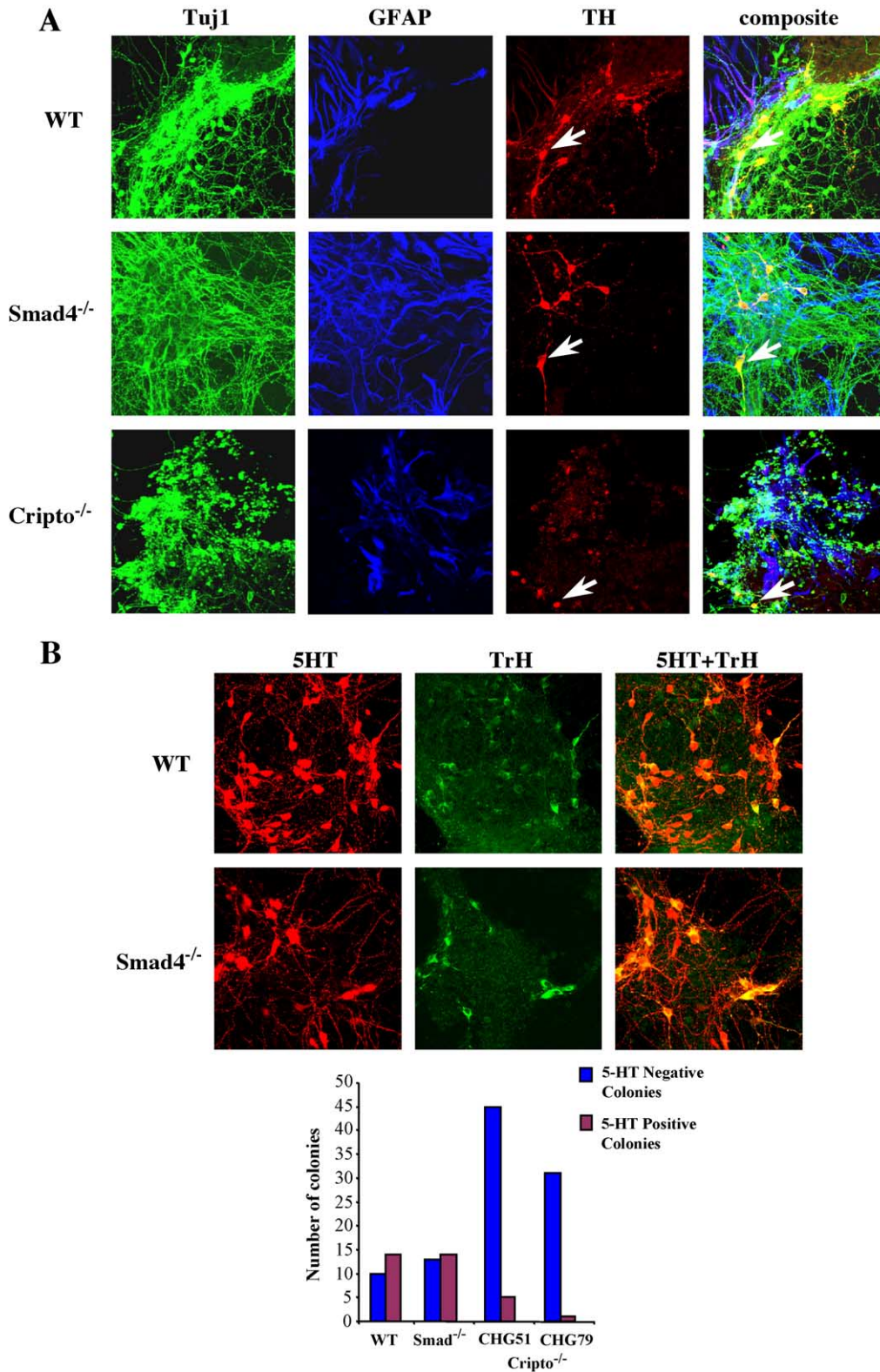


Fig. 5. Development of catecholaminergic neurons after in vitro differentiation. (A) Development of DA neurons. ICC for Tuj1 (green), GFAP (blue), and TH (red) after in vitro differentiation of WT (E14K), *Smad*^{-/-}, and *Cripto*^{-/-} ES cells. TH⁺/Tuj1⁺ neurons appear yellow in composite images and are shown by white arrows. (B) Development of serotonergic neurons. ICC for 5HT (red) and TrH (green) after differentiation of WT E14K and *Smad*^{-/-} ES cells. Coexpression of 5HT and TrH in cells (yellow) is shown in composite images. Quantification of serotonergic cells by counting 5HT-negative (blue bars) and 5HT-positive (red bars) neuronal colonies after differentiation of WT and mutant ES cells. Samples were analyzed with 40× magnification.

ment from multiple germ layers was observed in high dose ES cell grafts (Fig. 1), we transplanted 50×10^3 cells into the striatum of naive animals and analyzed grafts 4 weeks after transplantation. Both the WT and the mutant cells developed into either large or small graft sizes (40%, 52%, and 23.5% large grafts; 35%, 29%, and 23.5% small grafts; 25%, 19%, and 53% no grafts for WT, *Smad4*^{-/-}, and *Cripto*^{-/-} ES cells, respectively). Interestingly, stereology analyses revealed that smaller WT, *Smad4*^{-/-}, and *Cripto*^{-/-} grafts had a higher proportion of neuronal components ($81.0 \pm 15.1\%$, $91.2 \pm 6.0\%$, and $97.1 \pm 4.0\%$, respectively) when compared with corresponding larger surviving grafts ($61.5 \pm 27.2\%$, $69.3 \pm 25.8\%$, and $51.0 \pm 29.9\%$, respectively). Notably, there was a trend toward higher amounts of neurons in small *Smad4*^{-/-} and *Cripto*^{-/-} grafts when compared to WT grafts, but this was not statistically significant.

Initial morphological examination of transplants, particularly in the larger grafts, indicated that a variety of nonneuronal cells had developed. Sections were therefore stained with the ectodermal–epidermal marker Cytokeratin and the mesodermal marker Myosin (Fig. 6A), and scored for their presence (see Experimental methods for details). The principal cell type in the small grafts developed from all three ES cell lines was neuronal, while we failed to detect mesodermal or ectodermal cell types (Fig. 6B). In contrast, all larger grafts had significant amounts of ectodermal–epidermal and mesodermal cells. To examine if there were remaining immature ES cells, we stained grafts with SSEA1. Clusters of SSEA1⁺ cells (Fig. 6A) were found in most grafts regardless of the ES cell source

(Fig. 6B). Finally, we determined the presence of DA and serotonergic neuronal subtypes in the grafts (Fig. 6A). These analyses showed only minor differences in the amounts of TH and 5HT cells between small and large grafts (Fig. 6B). However, there was a trend toward more serotonergic cell development in the *Smad4*^{-/-} grafts when compared to WT transplants.

Discussion

We have used ES cells as a source for obtaining midbrain DA neurons for Parkinson's disease in vivo (Bjorklund et al., 2002; Deacon et al., 1998; Isacson et al., 2003). Although the ES cells spontaneously developed into functional DA neurons (Bjorklund et al., 2002), they also differentiated into other cells from all germ layers. Because teratoma formation is the expected outcome of transplanted wild-type ES cells (Cai and Rao, 2002), reducing the capacity for ES or neural precursors to differentiate into nonneuronal tissue is desirable for therapeutic neuronal grafts to optimize functional effects and to limit cell overgrowth (Bjorklund et al., 2002; Isacson et al., 2003). One way to overcome teratoma formation in ES cell transplantation settings is the abrogation of unwanted cell development using gene-manipulated ES cells. Based on the established role of members of the TGF- β gene family in brain development and neurogenesis (Munoz-Sanjuan and Brivanlou, 2002), we therefore examined the hypothesis that the *Smad4* and *Cripto* genes

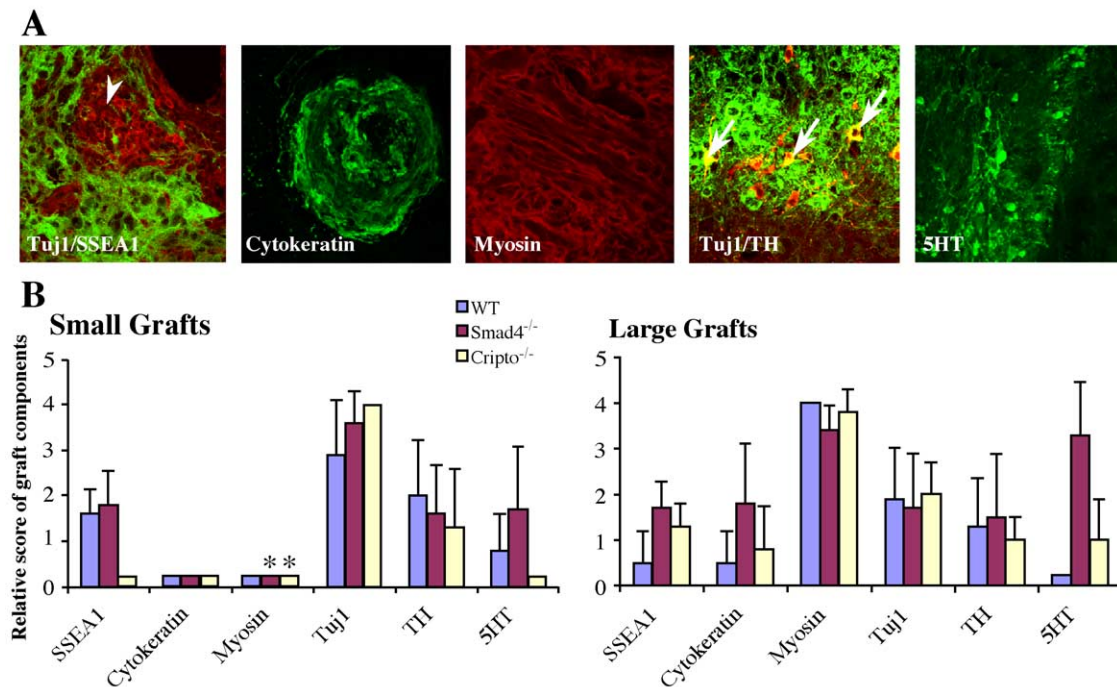


Fig. 6. Graft development and lineage specification of transplanted ES cells. (A) Confocal images from transplanted *Smad4*^{-/-} and *Cripto*^{-/-} ES cells 4 weeks after grafting. Cells developed into Myosin⁺ (red, *Cripto*^{-/-} graft) and Cytokeratin⁺ (green, *Smad4*^{-/-} graft) structures demonstrating mesodermal and ectodermal cell development. Note the typical “pearl”-like formation of Cytokeratin⁺ cells. Grafts also consisted of TH⁺ (red, *Cripto*^{-/-} graft) and 5HT⁺ (green, *Smad4*^{-/-} graft) neurons. TH⁺ neurons are costained with Tuji1 (green) and appear yellow (white arrows). SSEA1⁺ (red, *Smad4*^{-/-} graft) cells were also present in grafts and grew in small clusters (white arrow heads). All images were taken at 40 \times magnification. (B) Semiquantitative analyses of graft components in small and large grafts. Grafts were evaluated using the following scoring scheme: 0 = no cells (0%); 1 = very few (<5%); 2 = distributed (5–20%); 3 = regional (20–50%); 4 = dominant (>50%). The differences between the values for the individual grafts (WT, *Smad4*^{-/-} and *Cripto*^{-/-}) were statistically not significant ($P > 0.5$). Note that no Cytokeratin⁺ and Myosin⁺ cells were detected in small grafts from WT, *Smad4*^{-/-}, and *Cripto*^{-/-} ES cells. When compared to corresponding large grafts, this finding was statistical significant ($P < 0.05$) for *Smad4*^{-/-} and *Cripto*^{-/-} grafts.

may play a role in neural induction in ES cell differentiation. Our results show that neither mutation of the upstream (*Cripto*) nor downstream (*Smad4*) factor is sufficient to induce exclusive development of neural cells. In addition, loss of function of *Cripto* or *Smad4* can be partially rescued in a non- or atypical embryological environment, because both genetically modified ES cell lines retained their capacity to form ectoderm, endoderm, and mesoderm when transplanted to the brain. Interestingly, we found that deletion of *Cripto* results in a more severe phenotype than deletion of *Smad4*, because *Cripto*^{-/-} ES cells lacked at least some aspects of terminal mesoderm differentiation, suggesting that *Smad4* function can potentially be compensated by other factors and pathways, such as observed in *Xenopus* by *Smad4b* (*Smad10*) (Howell et al., 1999; LeSueur and Graff, 1999).

The role of Smad4 and Cripto and the default pathway of neural induction

In several animal models, such as frog (*Xenopus*), zebrafish, chick, and more recently in mouse, a default mechanism of neural induction has been proposed (Harland, 2000; Munoz-Sanjuan and Brivanlou, 2002; Wilson and Edlund, 2001). This model proposes that neural induction is initiated by the inhibition of BMP signaling in the embryonic ectoderm, through the normal activity of BMP inhibitors such as *noggin*, *chordin*, *folliculin*, and *twisted gastrulation*. In mouse ES cell differentiation, two lines of evidence are consistent with this model of neural induction: First, transplantation at low density of mouse ES cells into the striatum or under the kidney capsule of adult mice predominantly leads to the formation of neural (mid- and hindbrain) cell types (Deacon et al., 1998). Second, in vitro differentiation of mouse ES cells on stromal feeders (Kawasaki et al., 2000) or in limiting dilution assays (Tropepe et al., 2001) results in development of neural cell populations. In these in vitro experiments, the ES cells rapidly acquire a neural cell fate when differentiated at low cell density and/or when BMP signaling is inhibited by BMP antagonists or by deletion of the *Smad4* gene. However, these experiments were based on the generation of neural precursors from ES cells in the absence of EB formation, therefore preventing early cell–cell contact and a cellular environment for the promotion of germ layer development. In the present study, we tested whether the deletion of *Smad4* or *Cripto* is sufficient to induce neural differentiation even in the presence of germ layer formation and cell–cell contact. In contrast to the work of Tropepe et al., we did not culture the ES cells in low densities and also allowed the formation of EBs in our in vitro differentiation protocol. We found an increase in neurogenesis. We also found that the cells could differentiate into multilineage cell types, demonstrating that loss of function of *Smad4* and *Cripto* was not sufficient to result in a default pathway of neural differentiation in this in vitro paradigm. These results were also substantiated by the in vivo transplantation experiments, which showed differentiation of multiple cell types in ES cell-derived grafts regardless of their WT, *Smad4*^{-/-}, or *Cripto*^{-/-} profile. However, we also observed small grafts, which consisted entirely of neurons, suggesting that some circumstances may predispose toward neural specification. As recently reported and summarized in the present study, transplanted ES cells in the striatum often developed into large grafts with cells from all germ layers

when implanted at high cell concentrations (Deacon et al., 1998), whereas transplantation at lower cell density facilitated neuronal differentiation (Bjorklund et al., 2002). These data suggest that factors like cell–cell contact and cellular and graft–host environment determine whether a developing ES cell follows a pathway of neural specification or differentiates into other nonneuronal phenotypes.

Differentiated Smad4^{-/-} and Cripto^{-/-} ES cells display midbrain and hindbrain gene expression profiles and can develop into catecholaminergic neurons

Smad4^{-/-} embryos die at E7.5, do not form mesoderm, and show abnormal visceral endoderm development, while in later developmental stages, they have abnormal headfolds and lack expression of the posterior hindbrain marker *Krox20* (Sirard et al., 1998; Weinstein et al., 2000; Yang et al., 1998). In our study, the in vitro differentiated *Smad4*^{-/-} ES cells showed an up-regulation of *En-1*, a marker of prospective midbrain and anterior hindbrain, during development when compared with the corresponding E14K WT, indicating that expression of marker genes of the anterior hindbrain were not inhibited by lack of *Smad4*. *Cripto*^{-/-} embryos show widespread expression of the forebrain and midbrain marker *Otx2* and also express *En-1* (Ding et al., 1998). In addition, *Cripto*^{-/-} embryos express the rostral hindbrain marker *Gbx2* in early ectoderm development (Kimura et al., 2001). It is of interest to note that in *Cripto*^{-/-} embryos, the relative position of the anterior neural territories, i.e., the isthmic organizer and the caudal midbrain, is conserved and that markers of midbrain neuronal development including *Wnt1* and *Fgf8*, but not sonic hedgehog (*Shh*) (Ding et al., 1998), are expressed (Liguori et al., 2003). In our in vitro differentiation experiments, *Cripto*^{-/-} ES cells demonstrated similar expression patterns of *Otx2* and *En-1* when compared to the WT TC1 ES cells, indicating that the knockout cell lines retained their ability to express anterior brain and midbrain markers. However, in contrast to the WT, the *Cripto*^{-/-} ES cells expressed *Gbx2* at late stages of cell development. This is consistent with the notion that *Cripto* might be involved in the suppression of *Gbx2* (Kimura et al., 2001).

Based on the observation that ES cells can differentiate in vitro and in vivo into midbrain DA and serotonergic neurons (Barberi et al., 2003; Bjorklund et al., 2002; Chung et al., 2002; Deacon et al., 1998; Kawasaki et al., 2000; Kim et al., 2002; Lee et al., 2000), we also determined whether the *Smad4*^{-/-} and *Cripto*^{-/-} ES cells could generate catecholaminergic neurons. Our results demonstrate that both the *Smad4*^{-/-} and the *Cripto*^{-/-} ES cell lines had an up-regulation of DA-specific markers such as *Nurr1*, *TH*, *AADC*, *AHD2*, and *DAT* after in vitro differentiation and developed into comparable numbers of *TH*⁺ neurons in vitro and in vivo when compared to their corresponding WT ES cell lines. In addition, the *Smad4*^{-/-} and *Cripto*^{-/-} ES cells developed into *5HT*⁺/*TrH*⁺ neurons, indicating that the mutant ES cells retained their ability to differentiate into midbrain DA and serotonin neurons.

Loss of function of Smad4 and Cripto can be rescued in Smad4^{-/-} and Cripto^{-/-} ES cell differentiation

The shift toward neuroectoderm and the lack of mesoderm and endoderm in *Smad4*^{-/-} and *Cripto*^{-/-} mouse embryos suggests that in vitro and in vivo differentiation of their corresponding ES cells would have similar developmental outcomes. Here we show

that this is only partially the case. The *Smad4*^{-/-} cells showed endodermal marker gene expression at early (ES and EB), but not at late (NP and ND), developmental stages. In addition, they clearly had mesodermal gene expression at late stages as shown by RT-PCR for Brachyury and also developed into Myosin⁺ cells in the tissue cultures. These results are partly consistent with observations made by Sirard et al. showing that early and late visceral endodermal and mesodermal markers are absent in EBs at day 5 and day 7 of in vitro development, but present when EBs were grown for 12 days (Sirard et al., 1998). Taken together, these results demonstrate that mutating the *Smad4* signaling pathway is not sufficient to entirely block mesodermal (and endodermal) differentiation.

A slightly different picture was observed in the differentiation of *Cripto*^{-/-} ES cells. First, we observed an early (ES, EB, and NP), but not late (ND), increase in *HNF4* gene expression in the mutant cell line. Because *Nodal/Cripto* signaling has an essential role for the formation of definitive endoderm (Shen and Schier, 2000; Whitman, 2001), this result could imply that the *Cripto*^{-/-} cells produce extraembryonic visceral, but not definitive endoderm. Second, *Cripto*^{-/-} ES cells seemed to be able to express early mesoderm markers (Brachyury), but were defective in the differentiation of at least some terminal mesoderm (Myosin). This is consistent with results from *Cripto*^{-/-} mice, which lack embryonic mesoderm. However, in vivo differentiation of *Cripto*^{-/-} ES cells clearly demonstrated the production of terminally differentiated mesodermal cell types. One explanation could be that loss of the extracellular function of *Cripto* can be compensated more readily in the transplant condition by spatial constraints and by the host mouse adult striatum, thus activating the TGF- β receptors or alternative pathways in the grafted *Cripto*^{-/-} cells. To this end, RT-PCR analyses revealed the presence of *Cripto* transcripts in the adult brain and the striatum (data not shown). It is of interest to note that in the in vitro experiments, both the WT and the *Smad4*^{-/-} cells expressed *Cripto* only at early (ES and EB) stages of cell differentiation, suggesting that mesoderm differentiation may be dependent on the early expression of *Cripto*. These results are consistent with previous observations that *Cripto* may possess a dual role as a co-receptor or co-ligand for Nodal (Yan et al., 2002).

Taken together, our results demonstrate that loss of function of *Smad4* and *Cripto* can be compensated by in vitro and in vivo ES cell differentiation conditions. In addition, ES cell derived neurogenesis does not entirely depend on functional *Smad4* and *Cripto*, indicating that multiple factors are involved in the default mechanisms for neural fate specification, such as cell–cell contact, the cellular environment, and other extrinsic or intrinsic (signaling) molecules.

Experimental methods

ES cell culture and in vitro differentiation

Wild-type (WT) E14K, *Smad4*^{-/-} (C8-13A1) (kindly provided by Drs. C. Sirard and Tak W. Mak, University of Toronto, Toronto, Canada) and WT TC1, and the *Cripto*^{-/-} (clones CHG51 and CHG79) (kindly provided by Dr. M. M. Shen, UMDNJ-Robert Wood Johnson Medical School, New Jersey, USA) ES cells were propagated and in vitro differentiated as described previously (Chung et al., 2002; Lee et al., 2000).

Immunocytochemistry

Cells were analyzed by immunofluorescence staining as previously described (Chung et al., 2002) and examined using an LSM510 Meta confocal microscope equipped with ultraviolet, argon, and helium–neon lasers (Carl Zeiss, Thornwood, NY). The following primary antibodies were used: rabbit anti-glial fibrillary acidic protein (GFAP, Dako, Carpinteria, CA; 1:500), mouse anti- β -III-tubulin (Covance, Richmond, CA; 1:500), rabbit anti- β -III-tubulin (Covance; 1:2000), sheep anti-tyrosine hydroxylase; TH (Pel-Freez, Rogers, AK; 1:300), rabbit anti-TH (Pel-Freez; 1:300), mouse anti-TH (Pel Freez; 1:300), rabbit anti-serotonin (INCSTAR/#20080; 1:2500), sheep anti-tryptophan hydroxylase (Pel Freez; 1:300), mouse anti-Nestin (Developmental Studies Hybridoma Bank, Iowa City, IO; 1 μ g/ml), mouse anti-SSEA1 (Dev. Studies Hybridoma Bank; 1 μ g/ml), rabbit anti-Cytokeratin (Dako; 1:400), mouse anti-Myosin (MF20, Dev. Studies Hybridoma Bank; 1 μ g/ml). The secondary antibodies utilized were Alexa Fluor 488, 594, and 660 conjugated donkey immunoglobulin (Molecular Probes, Eugene, OR; 1:500).

RNA preparation and RT-PCR

Total RNA from plated cells at different stages in the differentiation protocol was prepared using TriReagent (Sigma) followed by treatment with DNase I (DNA-free, Ambion). For RT-PCR analysis, 3–5 μ g RNA was transcribed into cDNA with the SuperScript™ Preamplification Kit (Life Technologies) and oligo (dT) primers. The cDNA was then diluted 1:3 and 2.5% per reaction were analyzed in a PCR assay using the following mouse-specific primers:

β -actin: 5'-GGTGATGACCTGGCCGTCAGGCAGCTCGTA-3'; 5'-AACCCCAAGGCCAACCGCGAGAAGATG ACC-3' (402 bp)
 Nurr1: 5'-CATGGACCTCACCAACACTG-3'; 5'-GAGACAGGTGTCTTCCTCTG-3' (383 bp)
 TH: 5'-TCCTGCACTCCCTGTCAGAG-3'; 5'-CCAAGAGCAGCCCATCAAAGG-3' (423 bp)
 GBX2: 5'-GAGCATCACACAGGGTTCTG-3'; 5'-CACCTTAAATCGCGCTCCTC-3' (370 bp)
 Brachyury: 5'-ACAATTCATCTGCTTGCTGTGCC-3'; 5'-CGGTTGTTACAAGTCTCAGCAG-3' (436 bp)
 HNF-4: 5'-GAGGTCCATGGTGTAAAGGAC-3'; 5'-CTGCAGCAGGTTGTCAATCTTGG-3' (410 bp)
 GATA4: 5'-AGATGCGCCCCATCAAGACAG-3'; 5'-CCGGAACACCCATATCCTAAG-3' (413 bp)
 Tuj1: 5'-AACTATGTAGGGGACTCAGACCTGC-3'; 5'-TCTCACACTTTCCGCAGAC-3' (274 bp)
 Nodal: 5'-GAGGTGACCAAGCCACTCTCC-3'; 5'-AGGGT-TAGGACACTCGCCCTC-3' (407 bp)
Cripto: 5'-GCAACTGTGAACATGATGTTTCG-3'; 5'-TG-AGGTCCTGGTCCATCAGC-3' (174 bp).

The primer sequences for amplifying the following genes were previously published: *Otx2*, *En-1*, and *Nestin* (Lee et al., 2000), *Smad4* (Oxburgh and Robertson, 2002).

PCR reactions were carried out with 1 \times IN Reaction Buffer (Epicentre Technologies, Madison, WI), 1.4 nM of each primer, and 2.5 units of Taq I DNA polymerase (Promega, Madison, WI). Samples were amplified in an Eppendorf Thermocycler (Brink-

mann Instruments, Westbury, NY) under the following conditions: denaturing step at 95°C, 40 s; annealing step at 60°C, 30 s; amplification step at 72°C, 1 min for 25–35 cycles; and a final amplification step at 72°C, 10 min. For semiquantitative PCR, cDNA templates were normalized by amplifying actin-specific transcripts and levels of gene transcription were detected by adjusting PCR cycling and primer design in such a way that each primer set amplified its corresponding gene product at its detection threshold to avoid saturation effects. Twenty to forty percent of the PCR products were analyzed in 7% polyacrylamide gels. Gels were then stained with ethidium bromide and visualized under UV light and photographed on Polaroid 3000 black and white prints. Photographs were scanned with an Epson (Epson Perfection 1640SU) scanner.

For evaluation of levels of gene expression, signal intensities (optical densities, OD) were measured using the NIH image software program (National Institutes of Health, USA), version 1.61. After subtracting background signals, values were calculated as percentages of the corresponding actin signals. Each PCR was performed in triplicate and values for the mutant *Smad4*^{-/-} and *Cripto4*^{-/-} ES cell lines calculated as percent of corresponding values from the WT E14K and TC1 samples, respectively.

Preparation of ES cells for transplantation

ES cells were cultured for 4 days in the absence of LIF on 100-mm Fisher brand bacteriological-grade petri dishes to form embryoid bodies (EB). EBs were then transferred to 15-ml sterile culture tubes, spun at 1000 rpm for 5 min, and rinsed once in Ca²⁺ and Mg²⁺-free Dulbecco's phosphate-buffered saline (D-PBS, Gibco/BRL). After rinsing, D-PBS was removed and 1.5 ml of trypsin solution was added. The cells were incubated for 5 min at 37°C and triturated with fire-polished Pasteur pipettes with decreasing aperture size to fully dissociate the cells. Finally, ES cells were spun at 1000 for 5 min and the trypsin solution replaced with 200- μ l culture media. The viability and concentration of the ES cells was determined using a hemocytometer after staining with acridine orange and ethidium bromide.

Transplantation into mice

C57BL6 mice ($n = 68$: wild-type = 20, *Smad4*^{-/-} = 31, *Cripto*^{-/-} = 17) (25 g; Charles River, Wilmington, MA) were anesthetized with an i.m. injection of a mixture of ketamine (100 mg/kg, Ketaset, Fort Dodge, IA) and xylazine (5 mg/kg, Xyla-Ject, Phoenix Pharmaceuticals, St. Joseph, MO), and placed in a Kopf stereotaxic frame (David Kopf Instruments, Tujunga, CA) equipped with a mouse adapter. Each animal received an injection of 1.0 μ l (0.25 μ l/min) ES cell suspension into the striatum (from Bregma: A⁺ 1.0 mm, L^{-/+} 1.8 mm, V- 2.8 mm) using a 26-gauge, 10- μ l Hamilton syringe. After the injection of cells, we waited 2 min to allow the ES cells to settle before the needle was removed. After surgery, each animal received an intraperitoneal (i.p.) injection of Buprenorphine (0.032 mg/kg) as postoperative anesthesia.

Histological procedures

At 1, 2, 3, or 4 weeks after the implantation of ES cells, animals were terminally anesthetized by an i.p. injection of pentobarbital (100 mg/kg) and perfused intracardially with 70 ml heparin saline (0.1% heparin in 0.9% saline) followed by 100 ml paraformaldehyde

(4% in PBS). The brains were removed and postfixed for 8 h in the same 4% paraformaldehyde solution. Following postfixation, brains were equilibrated in sucrose (20% in PBS), sectioned (40 μ m) on a freezing microtome, and collected in PBS.

Immunohistochemistry

Sections were rinsed for 3 \times 10 min in PBS, preincubated in 4% normal donkey serum (NDS; Jackson Immunoresearch Laboratory) for 60 min, and then incubated overnight at room temperature with primary antibody diluted in PBS with 2% NDS and 0.1% Triton X-100. After additional rinsing 3 \times 10 min in PBS, the sections were incubated in fluorescent-labeled secondary antibodies (Cy2/Rhodamine Red-X/Cy5 labeled, raised in donkey; Jackson Immunoresearch Laboratory) in PBS with 2% NDS and 0.1% Triton X-100 for 60 min at room temperature. After rinsing 3 \times 10 min in PBS, sections were mounted onto gelatin-coated slides and coverslipped in Gel/Mount (Biomedica Corp., CA, USA).

Graft analyses

Design-based stereology was performed on the grafts using an integrated epifluorescent Axioskop-2 microscope (Carl Zeiss) and Stereo Investigator workstation (MicroBrightField, Williston, VT). Graft volumes were calculated using a Cavalieri estimator and the resultant coefficient of error estimate established data precision ($P < 0.05$). Grafts were classified in small and large grafts according to their size relative to striatum (25 mm³), whereby small grafts were smaller (<25 mm³) and large grafts larger (>25 mm³) than striatum (Figs. 1C and D). Estimation of cell components in grafts was performed using a semiquantitative scoring system. Grafts were stained by Immunohistochemistry, examined under the microscope, and scored by two to three independent investigators using the following criteria: 0 = no cells (0%); 1 = very few (<5%); 2 = distributed (5–20%); 3 = regional (20–50%); 4 = dominant (>50%).

Cell counting and statistical analyses

Cell populations in ND stage of in vitro differentiation were counted at 63 \times magnification, using a Zeiss Axioplan I fluorescent microscope, in randomly selected fields ($N = 16$ or more, as indicated). The cultures were also monitored at lower magnification (10 \times or 20 \times) to observe general growth pattern. Grafts were analyzed at 40 \times magnification and cell components scored as described above. For all statistical analyses including the values from the RT-PCR experiments, the JMP software (JMP Statistical Made Visual, Version 3, SAS Institute Inc., Cary, NC) was used for performing analysis of variance (ANOVA) with an α level of 0.01 to determine possible statistical differences between group means. When significant differences were found, post hoc analysis was performed using Fisher's PLSD ($\alpha = 0.05$).

Acknowledgments

We want to thank Anne Dwyer and Andrew Ferree for their excellent technical help. The WT E14K and *Smad4*^{-/-} (C8-13A1) ES cells were kindly provided by Drs. C. Sirard and Tak W. Mak (University of Toronto, Toronto, Canada). This work was supported by NIH grants (O.I.) (P50)N539793, MH48866,

DAMD-17-01-1-0762, DAMD-17-01-1-0763, and Kinetics Foundation and Parkinson's Foundation National Capital Area, by grants from the American Heart Association (J.D.), Leukemia and Lymphoma Society (J.D.), NCCR (COBRE grant P20-RR/DE17702) (J.D.), and NIH grant HD042837 (M.M.S.).

References

- Barberi, T., Klivenyi, P., Calingasan, N.Y., Lee, H., Kawamata, H., Loonam, K., Perrier, A.L., Bruses, J., Rubio, M.E., Topf, N., Tabar, V., Harrison, N.L., Beal, M.F., Moore, M.A., Studer, L., 2003. Neural subtype specification of fertilization and nuclear transfer embryonic stem cells and application in parkinsonian mice. *Nat. Biotechnol.* 21, 1200–1207.
- Bianco, C., Adkins, H.B., Wechselberger, C., Seno, M., Normanno, N., De Luca, A., Sun, Y., Khan, N., Kenney, N., Ebert, A., Williams, K.P., Sanicola, M., Salomon, D.S., 2002. Cripto-1 activates nodal- and ALK4-dependent and -independent signaling pathways in mammary epithelial cells. *Mol. Cell. Biol.* 22, 2586–2597.
- Bjorklund, L.M., Sanchez-Pernaute, R., Chung, S., Andersson, T., Chen, I.Y., McNaught, K.S., Brownell, A.L., Jenkins, B.G., Wahlestedt, C., Kim, K.S., Isacson, O., 2002. Embryonic stem cells develop into functional dopaminergic neurons after transplantation in a Parkinson rat model. *Proc. Natl. Acad. Sci. U. S. A.* 99, 2344–2349.
- Cai, J., Rao, M.S., 2002. Stem cell and precursor cell therapy. *Neuromol. Med.* 2, 233–249.
- Chung, S., Sonntag, K.C., Andersson, T., Bjorklund, L.M., Park, J.J., Kim, D.W., Kang, U.J., Isacson, O., Kim, K.S., 2002. Genetic engineering of mouse embryonic stem cells by Nurr1 enhances differentiation and maturation into dopaminergic neurons. *Eur. J. Neurosci.* 16, 1829–1838.
- Daley, G.Q., 2002. Prospects for stem cell therapeutics: myths and medicines. *Curr. Opin. Genet. Dev.* 12, 607–613.
- Deacon, T., Dinsmore, J., Costantini, L.C., Ratliff, J., Isacson, O., 1998. Blastula-stage stem cells can differentiate into dopaminergic and serotonergic neurons after transplantation. *Exp. Neurol.* 149, 28–41.
- Ding, J., Yang, L., Yan, Y.T., Chen, A., Desai, N., Wynshaw-Boris, A., Shen, M.M., 1998. Cripto is required for correct orientation of the anterior–posterior axis in the mouse embryo. *Nature* 395, 702–707.
- Dinsmore, J., Ratliff, J., Deacon, T., Pakzaban, P., Jacoby, D., Galpern, W., Isacson, O., 1996. Embryonic stem cells differentiated in vitro as a novel source of cells for transplantation. *Cell Transplant.* 5, 131–143.
- Evans, M.J., Kaufman, M.H., 1981. Establishment in culture of pluripotent cells from mouse embryos. *Nature* 292, 154–156.
- Harland, R., 2000. Neural induction. *Curr. Opin. Genet. Dev.* 10, 357–362.
- Hooper, M., Hardy, K., Handyside, A., Hunter, S., Monk, M., 1987. HPRT-deficient (Lesch–Nyhan) mouse embryos derived from germline colonization by cultured cells. *Nature* 326, 292–295.
- Howell, M., Itoh, F., Pierreux, C.E., Valgeirsdottir, S., Itoh, S., ten Dijke, P., Hill, C.S., 1999. *Xenopus* Smad4beta is the co-Smad component of developmentally regulated transcription factor complexes responsible for induction of early mesodermal genes. *Dev. Biol.* 214, 354–369.
- Isacson, O., Bjorklund, L.M., Schumacher, J.M., 2003. Toward full restoration of synaptic and terminal function of the dopaminergic system in Parkinson's disease by stem cells. *Ann. Neurol.* 53 (Suppl. 3), S135–S146. (discussion S146–138).
- Kawasaki, H., Mizuseki, K., Nishikawa, S., Kaneko, S., Kuwana, Y., Nakanishi, S., Nishikawa, S.I., Sasai, Y., 2000. Induction of midbrain dopaminergic neurons from ES cells by stromal cell-derived inducing activity. *Neuron* 28, 31–40.
- Kim, J.H., Auerbach, J.M., Rodriguez-Gomez, J.A., Velasco, I., Gavin, D., Lumelsky, N., Lee, S.H., Nguyen, J., Sanchez-Pernaute, R., Bankiewicz, K., McKay, R., 2002. Dopamine neurons derived from embryonic stem cells function in an animal model of Parkinson's disease. *Nature* 418, 50–56.
- Kimura, C., Shen, M.M., Takeda, N., Aizawa, S., Matsuo, I., 2001. Complementary functions of Otx2 and Cripto in initial patterning of mouse epiblast. *Dev. Biol.* 235, 12–32.
- Le Belle, J.E., Svendsen, C.N., 2002. Stem cells for neurodegenerative disorders: where can we go from here? *BioDrugs* 16, 389–401.
- Lee, S.H., Lumelsky, N., Studer, L., Auerbach, J.M., McKay, R.D., 2000. Efficient generation of midbrain and hindbrain neurons from mouse embryonic stem cells. *Nat. Biotechnol.* 18, 675–679.
- LeSueur, J.A., Graff, J.M., 1999. Spemann organizer activity of Smad10. *Development* 126, 137–146.
- Li, J., Ning, G., Duncan, S.A., 2000. Mammalian hepatocyte differentiation requires the transcription factor HNF-4alpha. *Genes Dev.* 14, 464–474.
- Liguori, G.L., Echevarria, D., Improta, R., Signore, M., Adamson, E., Martinez, S., Persico, M.G., 2003. Anterior neural plate regionalization in cripto null mutant mouse embryos in the absence of node and primitive streak. *Dev. Biol.* 264, 537–549.
- Martin, G.R., 1981. Isolation of a pleuripotent cell line from early mouse embryos cultured in medium conditioned by teratocarcinoma stem cells. *Proc. Natl. Acad. Sci. U. S. A.* 78, 7634–7638.
- Massague, J., Chen, Y.G., 2000. Controlling TGF-beta signaling. *Genes Dev.* 14, 627–644.
- Minchiotti, G., Parisi, S., Liguori, G.L., D'Andrea, D., Persico, M.G., 2002. Role of the EGF-CFC gene cripto in cell differentiation and embryo development. *Gene* 287, 33–37.
- Munoz-Sanjuan, I., Brivanlou, A.H., 2001. Early posterior/ventral fate specification in the vertebrate embryo. *Dev. Biol.* 237, 1–17.
- Munoz-Sanjuan, I., Brivanlou, A.H., 2002. Neural induction, the default model and embryonic stem cells. *Nat. Rev., Neurosci.* 3, 271–280.
- Nagy, A., Rossant, J., Nagy, R., Abramow-Newerly, W., Roder, J.C., 1993. Derivation of completely cell culture-derived mice from early-passage embryonic stem cells. *Proc. Natl. Acad. Sci. U. S. A.* 90, 8424–8428.
- Oxburgh, L., Robertson, E.J., 2002. Dynamic regulation of Smad expression during mesenchyme to epithelium transition in the metanephric kidney. *Mech. Dev.* 112, 207–211.
- Persico, M.G., Liguori, G.L., Parisi, S., D'Andrea, D., Salomon, D.S., Minchiotti, G., 2001. Cripto in tumors and embryo development. *Biochim. Biophys. Acta* 1552, 87–93.
- Rhinn, M., Brand, M., 2001. The midbrain–hindbrain boundary organizer. *Curr. Opin. Neurobiol.* 11, 34–42.
- Rossi, F., Cattaneo, E., 2002. Opinion: neural stem cell therapy for neurological diseases: dreams and reality. *Nat. Rev., Neurosci.* 3, 401–409.
- Schier, A.F., Talbot, W.S., 2001. Nodal signaling and the zebrafish organizer. *Int. J. Dev. Biol.* 45, 289–297.
- Shen, M.M., Schier, A.F., 2000. The EGF-CFC gene family in vertebrate development. *Trends Genet.* 16, 303–309.
- Sirard, C., de la Pompa, J.L., Elia, A., Itie, A., Mirtsos, C., Cheung, A., Hahn, S., Wakeham, A., Schwartz, L., Kern, S.E., Rossant, J., Mak, T.W., 1998. The tumor suppressor gene Smad4/Dpc4 is required for gastrulation and later for anterior development of the mouse embryo. *Genes Dev.* 12, 107–119.
- Soudais, C., Bielinska, M., Heikinheimo, M., MacArthur, C.A., Narita, N., Saffitz, J.E., Simon, M.C., Leiden, J.M., Wilson, D.B., 1995. Targeted mutagenesis of the transcription factor GATA-4 gene in mouse embryonic stem cells disrupts visceral endoderm differentiation in vitro. *Development* 121, 3877–3888.
- Tiedemann, H., Asashima, M., Grunz, H., Knochel, W., 2001. Pluripotent cells (stem cells) and their determination and differentiation in early vertebrate embryogenesis. *Dev. Growth Differ.* 43, 469–502.
- Tropepe, V., Hitoshi, S., Sirard, C., Mak, T.W., Rossant, J., van der Kooy, D., 2001. Direct neural fate specification from embryonic stem cells: a primitive mammalian neural stem cell stage acquired through a default mechanism. *Neuron* 30, 65–78.
- Weinstein, M., Yang, X., Deng, C., 2000. Functions of mammalian Smad genes as revealed by targeted gene disruption in mice. *Cytokine Growth Factor Rev.* 11, 49–58.

- Weissman, I.L., 2000. Translating stem and progenitor cell biology to the clinic: barriers and opportunities. *Science* 287, 1442–1446.
- Whitman, M., 2001. Nodal signaling in early vertebrate embryos: themes and variations. *Dev. Cell* 1, 605–617.
- Wilkinson, D.G., Bhatt, S., Herrmann, B.G., 1990. Expression pattern of the mouse *T* gene and its role in mesoderm formation. *Nature* 343, 657–659.
- Wilson, S.I., Edlund, T., 2001. Neural induction: toward a unifying mechanism. *Nat. Neurosci.* 4, 1161–1168.
- Wrana, J.L., 2000. Regulation of Smad activity. *Cell* 100, 189–192.
- Yan, Y.T., Liu, J.J., Luo, Y.E.C., Haltiwanger, R.S., Abate-Shen, C., Shen, M.M., 2002. Dual roles of Cripto as a ligand and coreceptor in the nodal signaling pathway. *Mol. Cell. Biol.* 22, 4439–4449.
- Yang, X., Li, C., Xu, X., Deng, C., 1998. The tumor suppressor SMAD4/DPC4 is essential for epiblast proliferation and mesoderm induction in mice. *Proc. Natl. Acad. Sci. U. S. A.* 95, 3667–3672.